Int. J. Microgravity Sci. Appl., 33 (3) (2016) 330305
DOI: 10.15011/jasma.33.330305

IIIII ISPS-6 Proceedings IIIII
(Original Paper)

Stack Performance of Proton Exchange Membrane Based Unitized Reversible Fuel Cells

Hiroshi ITO[1], Naoki MIYAZAKI[2], Masayoshi ISHIDA[2] and Akihiro NAKANO[1]

Abstract

Proton exchange membrane (PEM) based unitized reversible fuel cells (URFCs) have attractive features as a key component of hydrogen utilization systems. To determine if drawbacks that do not appear in a small-scale single cell of a URFC are significant when a URFC has larger cells in a stack configuration required for commercial applications, a pilot-scale URFC system was successfully operated in both the electrolysis and fuel cell operation modes and both its overall stack performance and the performance variation between cells were measured. No significant drawbacks due to larger cells or stacking were detected in either mode. Local hydrogen pressure at the generation point during electrolysis mode and local flooding during fuel cell mode is examined based on experimental data.

Keyword(s): Unitized reversible fuel cell, Proton exchange membrane, Pilot-plant, Local hydrogen pressure, Local flooding
Received 24 December 2015, Accepted 8 June 2016, Published 31 July 2016

1. Introduction

Recently, hydrogen is attracting attention as an energy carrier for the temporary storage buffer of intermittent renewable energy, such as solar and wind[1)]. For this purpose, hydrogen is typically produced by a water electrolyzer powered by a renewable energy source (RES), such as a photovoltaic system or wind turbine, and is then stored in various forms, such as compressed, metal hydride, or liquefied. Such stored hydrogen can be used as fuel for power generation devices such as fuel cells. Hydrogen utilization systems composed of an electrolyzer, storage apparatus, and fuel cell have been studied by many countries for several decades. Compared with secondary batteries, hydrogen storage has several advantages in its high energy density and long-term stability.

In typical operation of a hydrogen utilization system, there is no overlap time between its two operation modes, electrolysis (EL) and fuel cell (FC) modes. A proton exchange membrane (PEM) electrolyzer and a proton exchange membrane fuel cell (PEMFC) both use a common PEM as the electrolyte, and have a similar cell/stack design. From a technical viewpoint, a unitized cell/stack of these two electrochemical devices is possible. Unitized reversible fuel cells (URFCs) based on a PEM have been studied for several decades[2-5)] as an energy device for space[6-8)] or terrestrial applications[9,10)]. As an energy-conversion device, URFCs have several advantages over the discrete installation of an electrolyzer and a fuel cell: 1) reduced cost of the total system, 2) higher operating ratio per individual device, 3) lower maintenance, and 4) smaller footprint.

In previous experimental studies[11-13)], we evaluated a URFC using a small-scale single cell of an URFC (electrode area of 27 cm^2) aiming to optimize cell components such as the gas diffusion layer (GDL) and flow channels in a bipolar plate. In a real-scale URFC system, each cell should have a larger electrode area (several hundred cm^2) and cells should be piled up into a stack. Drawbacks that did not appear in the small-scale single cell might be significant when larger cells are in a stack, such as nonuniform electrical contact in a catalyst layer (CL)/GDL- or GDL-bipolar plate, and the nonuniform distribution of gases and liquids due to partial closing of flow channels. These nonuniformities might produce current spots or overconcentration of reactant (liquids or gases), and consequently degrade the total stack performance. To determine if these drawbacks are significant when a URFC has larger cells in a stack configuration required for commercial applications, in this study, a pilot-scale URFC system was operated in both the EL and FC modes and then both its overall stack performance and the performance variation between cells were measured.

2. Principle of a Unitized Reversible Fuel Cell (URFC)

PEM electrolyzers and PEMFCs both are based on PEM technology and have a similar cell configuration, consisting of a membrane electrode assembly (MEA) including GDLs, and bipolar plates with flow channels. The fabrication method of MEAs can be divided into two categories based on the process used to apply the CL, that is, catalyst-coated membrane (CCM) and catalyst-coated substrate (CCS)[14)]. In fabricating a CL, inks or slurries containing catalyst are directly applied either to a GDL

1 National Institute of Advanced Industrial Science and Technology (AIST), 1-2-1 Namiki, Tsukuba 305-8564, Japan.
2 University of Tsukuba, 1-1-1 Tennoudai, Tsukuba 305-8573, Japan.
(E-mail: ito.h@aist.go.jp)

substrate or a PEM. Applying the catalyst inks to a GDL substrate forms a two-layer structure called a CCS, whereas applying to both sides of the PEM forms a three-layer structure called the CCM. Two CCSs are combined either with a PEM or with one CCM sandwiched between two GDLs, thus forming a five-layer MEA. Nowadays, an MEA for a PEMFC is commonly fabricated using the CCM process, whereas either the CCM or CCS process is used for a PEM electrolyzer. The configuration of a URFC with a PEM is the same as these PEM-based devices. Either process of CL application can be used to fabricate an MEA of a URFC.

A schematic of reactant/product transport during both operation modes of a URFC is shown in **Fig. 1**. In the EL mode, the following reactions occur at both electrodes by electric power input from the source.

$$2H^+ + 2e^- \rightarrow H_2\,(g) \quad \text{at cathode} \tag{1}$$

$$H_2O\,(l) \rightarrow 1/2O_2\,(g) + 2H^+ + 2e^- \quad \text{at anode} \tag{2}$$

The overall reaction thus can be expressed as,

$$H_2O\,(l) \rightarrow H_2\,(g) + 1/2O_2\,(g) \tag{3}$$

Liquid water is supplied to the anode as fuel (reactant) for the electrolysis, where it is dissociated into molecular oxygen (O_2), protons (H^+), and electrons (e^-). Protons formed at the anode migrate through the PEM to the cathode where they are reduced to molecular hydrogen (H_2). In this migration, water molecules (H_2O) accompany the migrating protons due to electro-osmotic drag. Thus, the PEM is kept wet without an outside water supply to the cathode, and therefore water as a reactant is supplied only at the anode during typical EL operation.

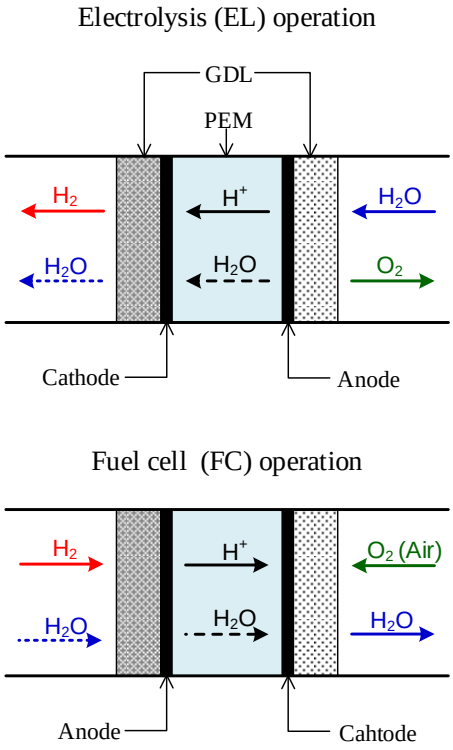

Fig. 1 Schematic of each operation of URFC: electrolysis (EL) mode and fuel cell (FC) mode.

In the FC mode, because reduction and oxidation at each electrode are reversed from that in the EL mode, the role of anode/cathode is also reversed, namely, the H_2 and O_2 electrode, respectively. H_2 and O_2 are respectively supplied to the anode and cathode, and then oxidized and reduced as follows.

$$H_2\,(g) \rightarrow 2H^+ + 2e^- \quad \text{at anode} \tag{4}$$

$$1/2O_2\,(g) + 2H^+ + 2e^- \rightarrow H_2O\,(l) \quad \text{at cathode} \tag{5}$$

The overall reaction during FC operation is completely opposite that during EL as follows:

$$H_2\,(g) + 1/2O_2\,(g) \rightarrow H_2O\,(l) \tag{6}$$

To maintain a sufficiently high proton conductivity of the PEM, the PEM has to be hydrated. The reactants of H_2 and O_2 are thus humidified during transport to the cell. Equation (5) shows, however, that liquid water is generated at the cathode. Excess liquid water would then accumulate at the CL/GDL interface and thus cause severe degradation of the cell performance because O_2 transport to the CL is hindered by accumulated water, which is called "flooding". Because FC performance is sensitive to the hydration state of the PEM and CL, the amount and state (liquid/vapor) of water in the cell must be carefully managed for stable operation.

3. Experimental Apparatus

The URFC stack and its balance of plants (BOP) were designed and manufactured by Takasago Thermal Engineering Co. (Japan). All components were enclosed in a cabinet (1,280 mm width × 740 length × 1,361 height mm); URFC stack, a pipeline system for gas and liquid including gas-liquid separators, valves, pumps, an air-blower, a control system including a control panel, a DC-power supply, an electric load, and a chiller.

3.1 URFC Stack

Figure 2 shows a schematic of the stacking configuration of the cells. (Not shown are the sealing components such as gasket and manifold.) In the cells in the present URFC stack, the MEAs were fabricated using the CCM process, and thus a composite of CCM sandwiched between two GDLs served as the MEA. As shown in **Fig. 2**, the MEA was rectangular with an area of 250 cm^2, and 10 cells were piled up to form a stack. **Table 1** lists the

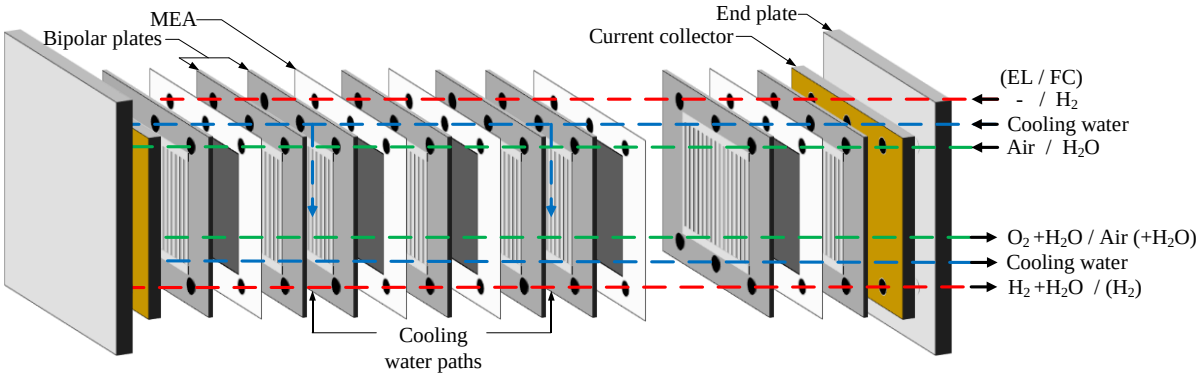

Fig. 2 Stacking configuration of cells in URFC.

specifications of an individual cell and of the stack. The total weight of this stack including both end-plates (made of stainless steel) was about 55 kg. The stack temperature (T_{stack}) was measured with a sheathed thermocouple (Type T) inserted into the body of one end-plate, with the tip of the sheath placed at the center of the electrode area. The stack had six fluid connections at one of the end-plates (right-hand side in **Fig. 2**), that is, the inlet and outlet lines for each fluid of H_2, O_2 (or air), and cooling water. Each fluid line passed through the bipolar plates and membranes. Each gas (H_2 and O_2 (or air)) was distributed to one side of each cell by using manifolds. Carbon, which is a typical material for the GDL and bipolar plate for a PEMFC, cannot be used for the oxygen electrode of a URFC (i.e., the cathode in the FC mode), because the potential of the oxygen electrode during EL mode is so cathodic that carbon material tends to corrode. Therefore, in the present URFC, a titanium (Ti)-felt was applied as the oxygen-electrode GDL, whereas carbon paper, which is a typical GDL substrate of a PEMFC, was used as the hydrogen-electrode GDL. For the bipolar plate, to facilitate the cooling-water path between the cells, two plates must be placed back-to-back. In this case, the potential of these two plates must be equal due to sufficient surface contact. Because the bipolar plates simultaneously function both as a cathode and anode, all bipolar plates must be resistant against high cathodic potential. Therefore, all the bipolar plates equipped here were made of Ti. However, Ti bipolar plates are costly, typically accounting for half the total cost of the stack[15]. Therefore, to reduce the number of bipolar plates, in our system, two bipolar plates (i.e., cooling water path) were placed only between every other cell (rather than between each cell) as shown in **Fig. 2**. Each bipolar plate had a terminal to measure the cell voltage.

Table 1 Specifications of URFC stack.

Material		
Membrane		Nafion 115
Catalyst	H_2 side	Pt
	O_2 side	Pt+IrO_2
Gas diffusion layer (Current collector)	H_2 side	Carbon paper
	O_2 side	Titanium felt
Bipolar plate		Titanium (Pt coated)
Cell/Stack configuration		
Electrode active area		250 cm^2
Number of cells in series		10

3.2 Balance of Plant (BOP)

There were six major line systems: inlet and outlet lines of H_2, inlet and outlet lines of air/O_2, electrolysis-water circulation line, and cooling-water circulation line. The outlet line of H_2 and part of the outlet line of air/O_2 were used for both EL and FC modes.

In the EL mode, deionized (DI) water stored in the O_2-water separator tank was fed into the URFC stack using a circulation pump for electrolysis water. Along with liquid water, the produced oxygen at the anode by electrolysis was released from the stack and fed back to the separator tank to remove the water. Oxygen gas was released from the tank and exhausted to the atmosphere. Simultaneously, hydrogen was produced at the cathode. Because liquid water migrated from the anode (O_2 side) to the cathode (H_2 side) through the membrane by electro-osmosis drag during electrolysis, hydrogen gas was also released with liquid water. Hydrogen was separated from the liquid water at the H_2-water separator tank and finally dried by cooling with a heat exchanger. Hydrogen pressure (P_{H2}) was regulated with a back pressure valve in the range between 0.1 to 1.0 MPa (abs). Because the line pressure of the oxygen side was always slightly higher than 0.1 MPa, a differential pressure existed between the anode and cathode when hydrogen was compressed at the anode.

In the FC mode, H_2 gas was supplied to the anode and air to the cathode. Note that the anode and cathode during FC mode are

opposite that during EL mode as shown in **Fig. 1**. In the recirculation system for the H_2 gas supply, residual H_2 released from the stack was recirculated with a recirculation pump. The flow rate of recirculated H_2 was fixed at 25 L/min, which corresponds to a stoichiometric ratio of 2.9 at current density of 0.5A cm^{-2}. To maintain a sufficiently high hydrogen purity, the recirculation line was opened at a moment (e.g., 1 sec) and hydrogen was fully recharged every 5 min. The stoichiometric ratio of H_2 was nearly 1. Air was supplied by an air blower (BLW) and was humidified with a membrane humidifier during transport to the stack. The membrane humidifier acted as a moisture exchanger between the air inlet and outlet lines, that is, by transferring moisture from the exhausted air containing higher m oisture to the inlet air. The flow rate of air was fixed at 48 L/min, and the dew point of introduced air at this flow rate was about 60 °C.

During both EL and FC modes, T_{stack} of the URFC was controlled using circulating cooling water. In this cooling-water loop, when T_{stack} reached a target temperature, cold water was supplied to the heat exchanger from the chiller. The temperature of the cooling water was measured at the inlet and outlet of the stack, and this temperature difference was then used to calculate the extracted thermal energy.

Using this URFC system (the URFC stack and its BOP), the stack current (I_{stack}) – stack voltage (V_{stack}) characteristics were measured at various operating conditions for both modes of EL and FC. The cell voltage (V_{cell}) variations were also obtained at the same time.

4. Results and Discussion

The URFC stack performance measured under nominal operating conditions at various T_{stack} is summarized in **Table 2**. Under nominal operation condition for the EL mode stack current I_{stack} = 250 A, hydrogen pressure P_{H2} = 1.0 MPa), power input for electrolysis (W_{stack}) was about 4.4 kW, when the Faraday (current) efficiency was near 1. In the FC mode, I_{stack} of nominal operation (i.e., the maximum I_{stack} for stable operation) was varied with T_{stack}. The maximum power output (W_{stack} = 0.8 kW) was obtained at T_{stack} = 70 °C and I_{stack} = 125 A. Details of the stack performance for both operation modes are described in the following sections.

4.1 Electrolysis (EL) Operation

The variable parameters for EL operation were T_{stack} and P_{H2}. **Figure 3** shows the measured I_{stack} – V_{stack} characteristics of EL under different T_{stack}, when P_{H2}=1.0 MPa. Because the overpotentials were relatively small during EL operation and the joule heat generated from the stack was lower than that during FC operation, T_{stack} was limited to under 60 °C. As expected, the EL performance was improved at higher T_{stack}, because the overpotential of both activation and ohmic decreased as T_{stack} was increased. The difference in V_{stack} (i.e., ΔV_{stack}) between different T_{stack} increased with increasing I_{stack}. Comparison of V_{stack} at T_{stack} = 40 and 60 °C shows that $\Delta V_{stack} \approx 1.0$ V at I_{stack} = 250 A, and thus the difference in W_{stack} for EL at these two temperatures was 0.25 kW. T_{stack} should be as high as possible to obtain a high stack

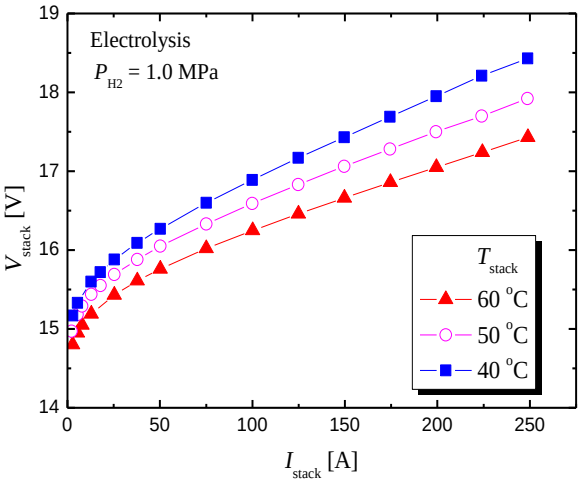

Fig. 3 Current (I_{stack}) – voltage (V_{stack}) characteristics of EL mode at various stack temperature (T_{stack}) at pressure of produced hydrogen (P_{H2}) of 1.0 MPa.

Table 2 Stack performance of URFC at nominal operating conditions.

Parameter		Electrolysis mode			Fuel cell mode	
Stack temperature	T_{stack} [ºC]	40	50	60	60	70
Stack current	I_{stack} [A]	250	250	250	100	125
Stack voltage	V_{stack} [V]	18.4	17.9	17.4	5.6	6.4
Stack power (DC)	W_{stack} [kW]	4.6	4.5	4.4	0.6	0.8
Hydrogen pressure (abs)	P_{H2} [MPa]	1.0	1.0	1.0	0.15	0.15
Produced/introduced hydrogen flow rate	F_{H2} [L/min]	17.4	17.4	17.4	7.2	8.9

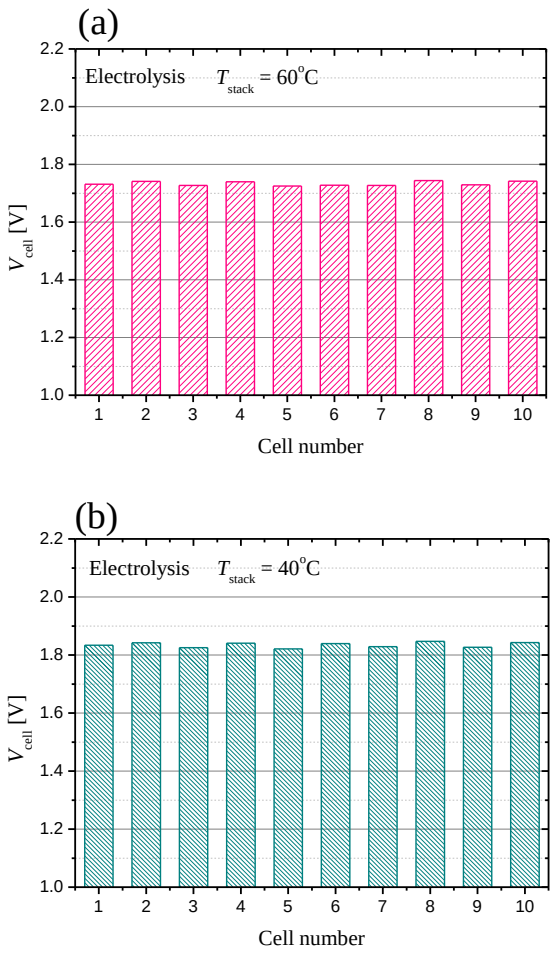

Fig. 4 Cell voltage (V_{cell}) variation during EL mode at (a) T_{stack} = 60 °C and (b) T_{stack} = 40 °C, when I_{stack} = 250 A and P_{H2}=1.0 MPa.

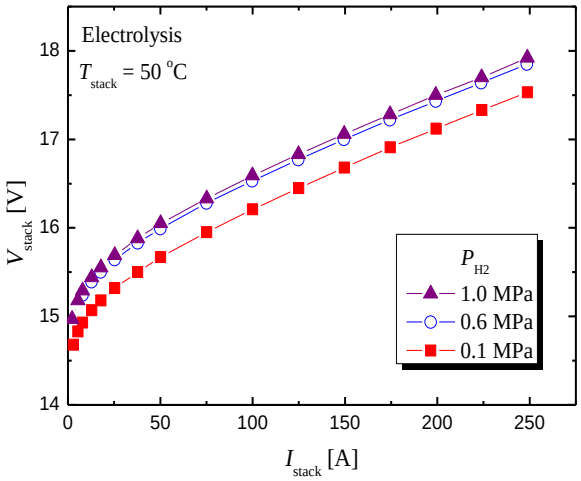

Fig. 5 I_{stack} –V_{stack} characteristics of EL mode at various P_{H2} at T_{stack} = 60 °C.

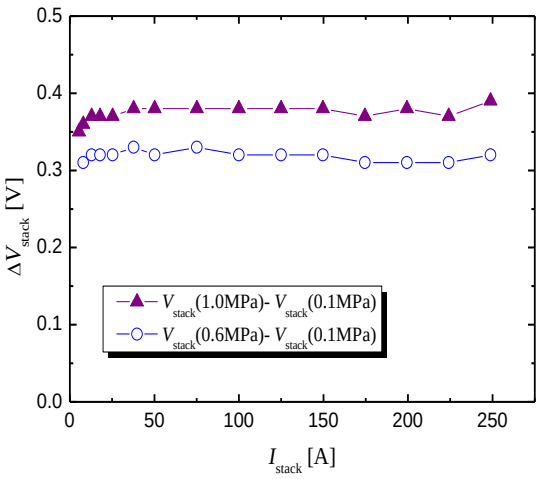

Fig. 6 Stack voltage difference (ΔV_{stack}) depending on the change in P_{H2}.

performance, though the maximum T_{stack} is around 80 °C due to the limitation of thermal stability of the PEM. The variation in cell voltage (V_{cell}) between the cells at T_{stack} = 40 and 60 °C is shown in **Fig. 4**, when P_{H2} = 1.0 MPa and I_{stack} = 250 A. At both levels of T_{stack}, the difference in V_{cell} between all 10 cells was very small. The maximum V_{cell} difference was 17 mV at T_{stack} = 40 °C and 22 mV at 60 °C. V_{cell} variations observed at other operating conditions (various T_{stack}, P_{H2}, and I_{stack}) reveal that V_{cell} difference during EL was small regardless of T_{stack}, P_{H2}, and I_{stack}. Consequently, no significant drawback due to larger cells or to stacking of the cells was observed in EL mode, that is, neither nonuniformity in the electric contact of CL-GDL and GDL-bipolar plates nor nonuniformity in the distribution of gases and liquids were observed.

Figure 5 shows the effect of P_{H2} on EL performance under the same T_{stack} (40 and 60 °C) The I_{stack} –V_{stack} performance at atmospheric P_{H2} (0.1 MPa) was better than that at higher P_{H2}, although the difference in performance between P_{H2} = 0.6 MPa and 1.0 MPa was relatively small. Based on the data in **Fig. 5**, **Fig. 6** is a plot of ΔV_{stack} between different P_{H2} versus I_{stack}. ΔV_{stack} was relatively independent of I_{stack}, and the I_{stack} –V_{stack} curve was shifted depending on the P_{H2} change, indicating negligible pressure dependency on overpotentials (activation and ohmic). Theoretical decomposition voltage of water (V_{EL_th}) can be derived from Eq. (3) as,

$$V_{EL\_th} = E_{rev} + \frac{RT}{2F}\ln\left(\frac{P_{H2}P_{O2}^{1/2}}{a_{H2O}}\right) \quad (7)$$

where E_{rev} is reversible potential of EL, R is gas constant, T is temperature of reaction field (i.e., T_{stack} in this case), F is the Faraday constant, P_{H2} and P_{O2} represent produced gas pressure of H_2 and O_2, respectively, and a_{H2O} is activity of reactant water. E_{rev}

can be derived from the Gibbs energy of Eq. (3)[16] and is 1.208 V at T=50 °C. If we assume EL under atmospheric conditions, then P_{H2}, P_{O2}, and a_{H2O} can be considered unity (i.e., $P_{H2} = P_{O2} = a_{H2O} = 1$), and thus the second term in the right-hand side in Eq. (7) would be zero. The V_{EL_th} due to pressure change from P_{H2} to P'_{H2} under constant temperature can be expressed as,

$$\Delta V_{EL\_th} = \frac{RT}{2F} \ln \frac{P'_{H2}}{P_{H2}} \quad (8)$$

Substituting T_{stack} (50 ºC) for T in Eq. (8), the calculated ΔV_{EL_th} is 25 mV at a P_{H2} change from 0.1 to 0.6 MPa, and as 32 mV at 0.1 to 1.0 MPa. The corresponding measured ΔV_{stack} in **Fig. 6** was on average 32 mV and 38 mV per cell, respectively. The measured P_{H2} represented an average pressure in the compressed hydrogen compartment, which is the region from the flow channel in the stack through the pipe to the back-pressure valve. The disagreement between the theoretical and measured voltage difference (ΔV_{EL_th} and ΔV_{stack}, respectively) suggests that the local hydrogen pressure at the hydrogen generation point in the electrode is significantly higher than P_{H2}, and the pressure difference between local and average would increase with increasing P_{H2}. If we assume the local hydrogen pressure at generation point under atmospheric pressure condition is equal to the average pressure (i.e., P_{H2}=0.1 MPa), the calculated P'_{H2} corresponding to measured ΔV_{stack} of 32 mV (at 0.1 to 0.6 MPa) and 38 mV (at 0.1 to 1.0 MPa) is 1.0 MPa and 1.5 MPa, respectively. These results indicate that the calculated local pressure was significantly higher than the average hydrogen pressure (i.e., measured P_{H2}).

4.2 Fuel cell (FC) Operation

Figure 7 shows the $I_{stack} - V_{stack}$ characteristics of the FC mode under T_{stack} = 70 and 60 °C. When I_{stack} > 50 A, a significant difference is evident. The rapid decrease in V_{stack} at T_{stack} = 60 °C indicates "flooding", that is, condensed liquid water in the cell/stack accumulated at the electrode and hindered the mass transport of reactive gases to the electrode surface. The dew point of air passing through the membrane humidifier was estimated at around 60 °C under the constant flow rate of the air regardless of T_{stack}. Therefore, the relative humidity (RH) of the air in the cathode gas channel would be around 100% when T_{stack} = 60 °C. **Figure 8** shows the variation in V_{cell} in all 10 cells during FC mode at current density of 0.4 A/cm^2 (i.e., 100 A). As shown in **Fig. 8a**, the difference in V_{cell} between the cells was small at T_{stack} = 70 °C, and the maximum difference was about 30 mV. Contrary to this, at T_{stack} = 60 °C (**Fig. 8b**), the difference in V_{cell} difference was large, and the maximum difference was about 300 mV, and cells of high V_{cell} alternated with those of low V_{cell}. The significant difference in V_{cell} observed at T_{stack} = 60 °C might be caused not by unexpected nonuniformity caused by larger cells or by

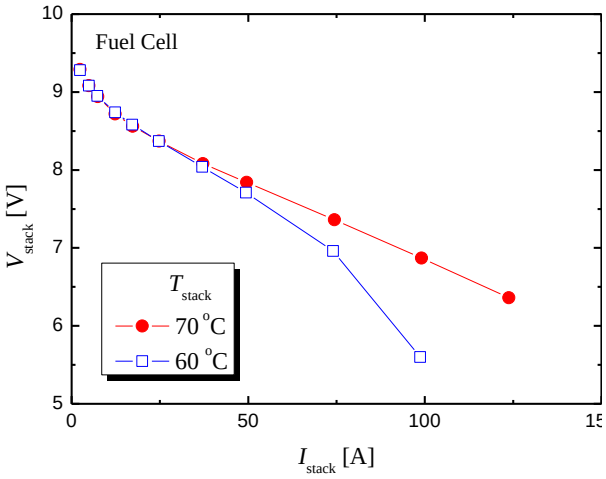

Fig. 7 $I_{stack} - V_{stack}$ characteristics of FC mode at different T_{stack}.

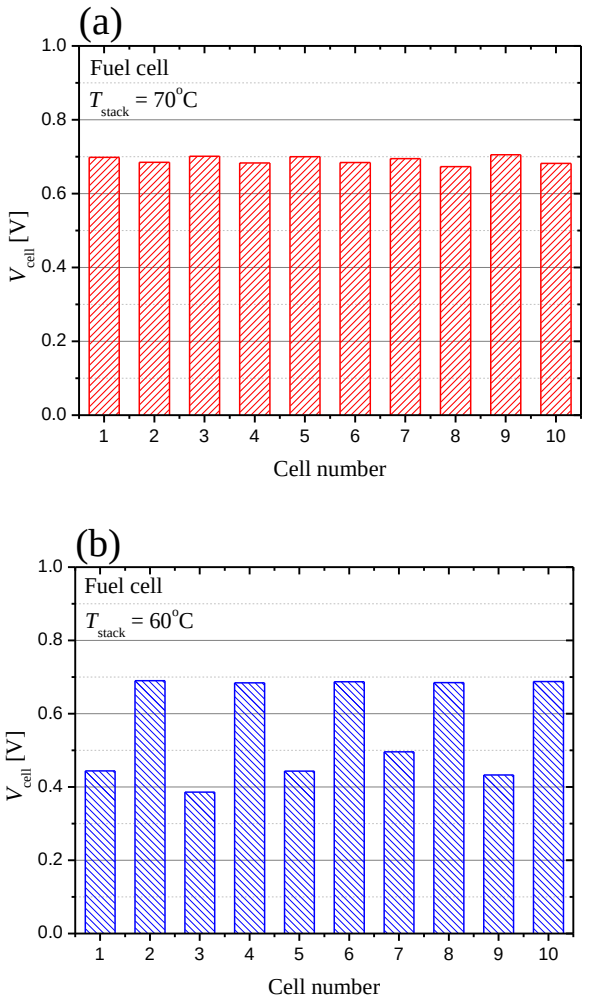

Fig. 8 Cell voltage variation during fuel cell operation at (a) T_{stack} = 70 °C and (b) T_{stack} = 60 °C, when I_{stack} = 100 A.

stacking of the cells but by the temperature difference between the cells. As mentioned above, each pair of cells in this stack configuration shared a common distribution of cooling water (see **Fig. 2**), and thus, there might be a temperature difference between the individual cells in each pair, although the temperature of each cell was not measured in the present experiments. The yield of flooding sensitively depends on RH. In the cells of lower temperature, RH of the air in the cathode gas channels would exceed 100 %. Because V_{cell} at this lower temperature would therefore be degraded due to severe flooding, V_{stack} would be degraded. Consequently, for FC mode, T_{stack} should be higher than 70 °C for stable operation with this URFC stack.

5. Conclusions

To determine if drawbacks that do not appear in a small-scale single cell of a URFC are significant when a URFC has larger cells in a stack configuration required for commercial applications, a pilot-scale URFC system was successfully operated in both EL and FC modes and both its overall stack performance and the performance variation between cells were measured.

In EL mode, the stack performance was improved by increasing T_{stack}. Experimental data revealed that the difference in V_{cell} between cells during EL is small regardless of T_{stack}, P_{H2}, and I_{stack}. Correspondingly, no significant degradation in stack performance due to enlargement or stacking of the cells was observed in EL operation. However, the effect of P_{H2} change on EL performance revealed that the local H_2 pressure at the hydrogen generation point in the electrode is significantly higher than the average of H_2 pressure in the compressed hydrogen compartment (the region from the flow channel in the stack through the pipe to the back-pressure valve).

In FC mode, the I_{stack}–V_{stack} curve at T_{stack} = 60 °C was severely degraded when I_{stack} > 50 A, significantly different from the I_{stack}-independent curve at T_{stack} = 70 °C. In addition, the difference in V_{cell} between the cells was significant at T_{stack} = 60 °C compared with that at 70 °C. This significant difference in V_{cell} observed at T_{stack} = 60 °C might be caused not by any unexpected defect due to larger cells or to stacking of the cells but by a temperature difference between the cells.

Acknowledgments

The authors gratefully acknowledge the financial support from the Ministry of Economy, Trade and Industry (METI) of Japan under the Japan-U.S. Cooperation Project for Research and Standardization of Clean Energy Technologies.

References

1) G. Gahleitner: Int. J. Hydrog. Energy, **38** (2013) 2039.
2) A.B. LaConti and L. Swette: Vielstich W, Lamm A, Gasteiger HA, editors. Handbook of fuel cells, John Wiley & Sons, **4** (2003) 745 (Ch. 55).
3) J. Pettersson, B. Ramsey and D. Harrison: J. Power Sources, **28** (2006) 157.
4) S.S. Dihrab, K. Sopian, M.A. Alghoul and M.Y. Sulaiman: Renew. Sust. Energy Rev., **13** (2009) 1663.
5) M. Gabbasa, K. Sopian, A. Fudholi and N. Asim: Int. J. Hydrog. Energy, **39** (2014) 17765.
6) R. Baldwin, M. Pham, A. Leonida, J. McElroy and T. Nalette: J. Power Sources, **29** (1990) 399.
7) F. Barbir, T. Molter and L. Dalton: Int. J. Hydrog. Energy, **30** (2005) 351.
8) Y. Sone: J. Power Sources, **196** (2011) 9076.
9) J.D. Maclay, J. Brouwer and G.S. Samuelsen: Int. J. Hydrog. Energy, **994** (2006) 31.
10) A. Kato, M. Masuda, A. Takahashi, T. Ioroi, M. Yamaki and H. Ito: ECS Trans., **1271** (2009) 25-1.
11) C.M. Hwang, M. Ishida, H. Ito, T. Maeda, A. Nakano, Y. Hasegawa, N. Yokoi, A Kato and T. Yoshida: Int. J. Hydrog. Energy, **36** (2011) 1740.
12) C.M. Hwang, M. Ishida, H. Ito, T. Maeda, A. Nakano, A Kato and T. Yoshida: J. Power Sources, **202** (2012) 108.
13) H. Ito, K. Abe, M. Ishida, C.M. Hwang and A. Nakano: Int. J. Hydrog. Energy, **40** (2015) 16565.
14) S.S. Kocha: Vielstich W, Lamm A, Gasteiger HA, Handbook of fuel cells, John Wiley Sons Ltd., **3** (2003) 538 (Ch. 43).
15) K.E. Ayers, E.B. Anderson, C.B. Capuano, B.D. Carter, L.T. Dalton, G. Hanlon, J. Manco and M. Niedzwiecki: ECS Trans., **3** (2010) 33-1.
16) R.L. LeRoy, C.T. Bowen and D.J. LeRoy: J. Electrochem. Soc., **127** (1980) 1954.